

and f is a rather complicated function expressed by

$$f(k_p a, \beta a) = \sum_{n=1}^{\infty} J_{2n+1}(2k_p a) \cdot \sum_{m=1}^n \left(\frac{m}{(\beta a)^2 - m^2} \right)^2 \quad (6)$$

Fig. 2 shows the variation of the preceding function in case of $\beta a \ll 1$. It can be shown that when $k_p a$ increases indefinitely,

$$f(k_p a, \beta a) \rightarrow \begin{cases} \frac{\pi^2}{8} \left[\csc^2(\pi \beta a) - \frac{1}{\pi \beta a} \cot(\pi \beta a) \right], & \beta a \neq 0 \\ \frac{\pi^2}{12} \simeq 0.8225, & \beta a = 0. \end{cases} \quad (7)$$

In Figs. 3 and 4 the radiation resistances given by (5) are plotted versus the radius of the loop and the plasma frequency for the case of $\beta = k_e$ (k_e is the propagation constant of the electromagnetic wave in an ambient plasma, i.e., $k_e = k_0(1 - \omega_p^2/\omega^2)^{1/2}$) and $k_p/k_e = c/u = 10^3$ (c is the light velocity).

On the other hand, the radiation resistance due to the electromagnetic wave radiation from the current distribution expressed by (3) with $\beta = k_e$ is obtained as follows:

$$R_e = \frac{1}{\pi} \sqrt{\frac{\mu_0}{\epsilon_0}} \left(1 - \frac{\omega_p^2}{\omega^2} \right)^{-1/2} \tan^2 k_e a \pi \cdot \sum_{n=0}^{\infty} J_{2n+1}(2k_e a) \cdot \left[\frac{(k_e a)^3}{(k_e a + n + 1)^2 (k_e a - n - 1)^2} - \frac{(k_e a)^3}{(k_e^2 a^2 - n^2)^2} + \sum_{m=1}^{2n+1} \frac{1}{k_e a + n - m + 1} \right] \quad (8)$$

and is also plotted in Figs. 3 and 4 to compare with the radiation resistance due to the plasma-wave radiation.

In a special case of a very small loop which satisfies the inequalities, $k_p a \ll 1$ as well as $\beta a \ll 1$, the radiation impedances due to the plasma wave and the electromagnetic wave radiations are given by

$$Z_p \simeq \frac{\pi}{3} \sqrt{\frac{\mu_0}{\epsilon_0}} (k_0 a)^2 (\beta a)^4 \left(\frac{c}{u} \right)^3 \left(\frac{\omega_p}{\omega} \right)^2 \cdot \left(1 - \frac{\omega_p^2}{\omega^2} \right)^{1/2} - j \frac{\pi^2}{2} \sqrt{\frac{\mu_0}{\epsilon_0}} \cdot (k_0 a)^2 \left(\frac{\omega_p^2}{\omega} \right)^2 \left(1 - \frac{\omega_p^2}{\omega^2} \right)^{1/2} \quad (9)$$

$$Z_e \simeq \frac{\pi}{6} \sqrt{\frac{\mu_0}{\epsilon_0}} (k_0 a)^4 \left(1 - \frac{\omega_p^2}{\omega^2} \right)^{3/2} + j \sqrt{\frac{\mu_0}{\epsilon_0}} k_0 a \left(\ln \frac{8a}{\rho} - 2 \right) \quad (10)$$

where ρ is the wire radius of the loop.

It is of interest to know the radius of the loop which radiates the same amounts

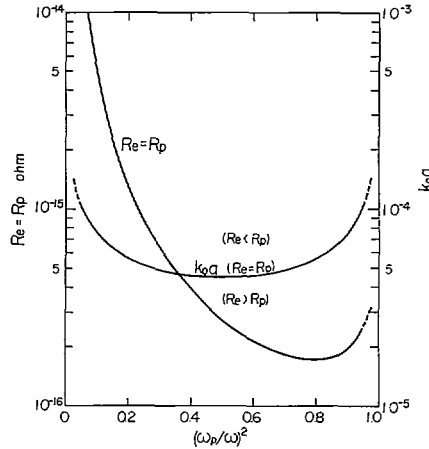


Fig. 5. Radius of loop which satisfies relation $R_e = R_p$ and radiation resistance, $k_p/k_e = 10^3$.

of the plasma wave power and the electromagnetic wave power, namely, satisfies the condition $R_p = R_e$. From (9) with $\beta = k_e$ and (10) the radius and the radiation resistance of such a loop is obtained as follows:

$$k_0 a = \left\{ 2 \left(\frac{c}{u} \right)^3 \left(\frac{\omega_p}{\omega} \right)^2 \left(1 - \frac{\omega_p^2}{\omega^2} \right) \right\}^{-1/2} \quad (11)$$

$$R_e = R_p = 5\pi^2 \left(\frac{c}{u} \right)^{-6} \cdot \left(\frac{\omega_p}{\omega} \right)^{-4} \left(1 - \frac{\omega_p^2}{\omega^2} \right)^{-1/2} \quad (12)$$

Note that the radius of the loop given by (11) satisfies the necessary condition $k_p a \ll 1$, except the case where ω_p/ω is extremely small. Fig. 5 illustrates the relations mentioned previously.

Finally, the far longitudinal electric field associated with the electron plasma wave is given by the following equation:

$$E_{pr} = \frac{1}{\pi} \sqrt{\frac{\mu_0}{\epsilon_0}} I_0 k_p a \sin \beta a \pi \left(\frac{\beta}{k_0} \right) \cdot \frac{\omega_p^2}{\omega^2 - \omega_p^2} \frac{e^{-jk_p r}}{r} \cdot \sum_{n=1}^{\infty} (-1)^{n+1} j^n J_n(k_p a \sin \theta) \cdot \frac{n}{\beta^2 a^2 - n^2} \sin n\phi. \quad (13)$$

It is obvious from the preceding equation that the plasma-wave radiation pattern of a small-loop antenna ($k_p a \ll 1$) is represented by the two spheres expressed by $\sin \theta \sin \phi$.

S. ADACHI
T. KASAHARA
Y. MUSHIAKE
Dept. of Elec. Comm. Engrg.
Tohoku University
Sendai, Japan

REFERENCES

- [1] K. J. Balmain, "Impedances of a short dipole, in a compressible plasma," *Radio Sci.*, vol. 69D, pp. 559-566, April 1965.
- [2] H. H. Kuehl, "Computations of the resistance of a short antenna in a warm plasma," *Radio Sci.*, vol. 2 (new ser.), pp. 73-76, January 1967.
- [3] J. R. Wait, *Electromagnetics and Plasmas*. New York: Holt, Rinehart and Winston, 1968.

Sheath Effects on the Current Distribution along an Antenna in a Plasma

Abstract—The sheath effects on the current distribution along a cylindrical antenna immersed in a plasma have been investigated in two respects: 1) the measurement and its interpretation of the current distribution of the antenna in the region of $f > f_p$ (f_p is plasma frequency) when its dc bias voltage is varied; 2) the observation and its interpretation of the slow-wave mode along the antenna in the region of $f < f_p/\sqrt{2}$.

INTRODUCTION

A number of theoretical papers have been published so far on the current distribution along a cylindrical antenna in a plasma. But very few papers [1], [2] on the experimental studies have been published. The present authors have measured the current distribution along a cylindrical monopole antenna immersed in a large scale plasma chamber surrounded by radio-wave absorbing walls and have found that the current distribution is essentially determined by the electromagnetic phase constant

$$k_e = k_0(1 - f_p^2/f^2)^{1/2}$$

(k_0 is a phase constant in free space) in the region of $f > f_p$, as already reported in the literature [1], [2]. In this communication some new experimental results and their theoretical interpretation concerning the sheath effects on the current distribution are reported. First, the variation of the current distribution was measured in the region of $f > f_p$, when a dc bias voltage was applied to the antenna insulated from the image plane. Second, the current distribution was measured in the cutoff region of the electromagnetic wave ($f < f_p$). As a result, a slow wave mode was observed in the region of $f < f_p/\sqrt{2}$. This mode is interpreted as a slow surface wave mode propagating along an ion-sheathed cylindrical conductor.

MEASURING SYSTEM

Fig. 1 illustrates the measuring system. The plasma was generated in a space surrounded by radio-wave absorbing walls which were set up in the space chamber of the Research Institute of Electrical Communication, Tohoku University. The volume of this space is about $1.4 \times 1.4 \times 0.7$ cubic meters. A_r was used as a discharging gas. The pressure is usually fixed at about $6 \mu\text{Hg}$. A large volume of plasma is formed by the diffusion process of the plasma generated in the abnormal glow discharged by the cold cathode (the anode is grounded). The electron density was measured by using the Langmuir double probe and the millimeter-wave Fabry-Perot resonator simultaneously. The plasma density distribution obtained in this chamber was

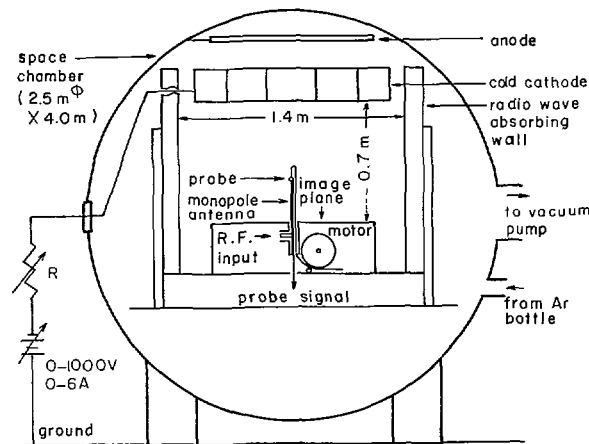
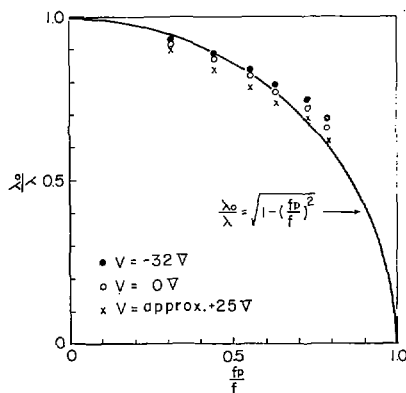
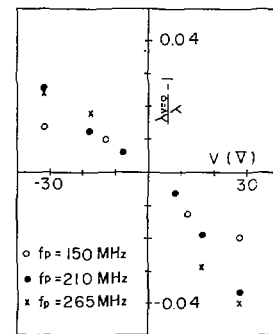
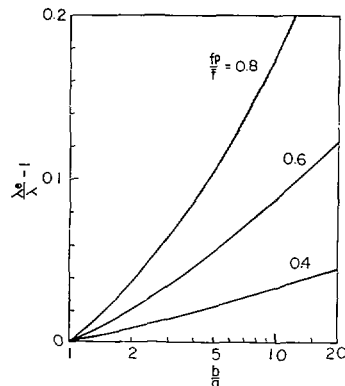
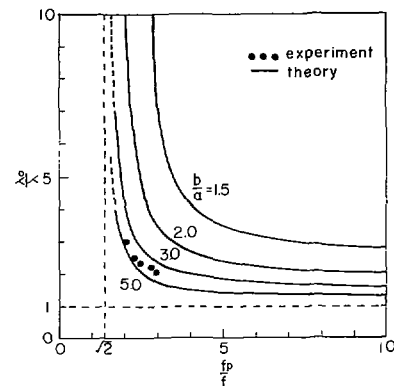


Fig. 1. Measuring system.

Fig. 2. Wavelength along antenna wire versus plasma frequency at different antenna bias voltages. $f = 485$ MHz.Fig. 3. Wavelength along antenna wire versus antenna bias voltage at different plasma frequencies. $f = 485$ MHz.Fig. 4. Propagation wavelength λ along cylindrical conductor versus sheath thickness at different plasma frequencies. $\lambda_0 = \lambda_0(1 - f_p^2/f^2)^{-1/2}$.Fig. 5. Wavelength along ion-sheathed cylindrical conductor versus plasma frequency in region of $f < f_p/\sqrt{2}$. $f = 108$ MHz.

found to be satisfactorily uniform in the horizontal direction but was not so uniform in the vertical direction as in the horizontal direction. A cylindrical monopole antenna with a length of 375 mm and a radius of 2.5 mm is situated at the center of the image plane with dimensions of 1×1 square meter. The current-measuring probe is driven by an electric motor and is moved along a longitudinal slot with a width of 1 mm on the antenna surface. The monopole antenna is insulated from the image plane in order to apply a dc bias voltage to it.

BIAS VOLTAGE AND CURRENT DISTRIBUTION

The monopole antenna was driven at the frequency of 485 MHz. The current distribution for various ambient plasma frequencies was measured when the dc bias voltage referred to the image plane is kept constant. It is expected that the ion sheath covering the antenna surface can be controlled by the applied dc bias. Thus the sheath effect on the current distribution can be experimentally studied. Fig. 2 shows the measured wavelength λ along the antenna referred to the free-

space wavelength λ_0 versus f_p normalized by the driving frequency f . The wavelength along the antenna was measured as four times the distance from the end of the antenna wire to the point of maximum current. Fig. 2 indicates that the wavelength on the wire has a tendency of variation, expressed by $\lambda_0/\lambda = \sqrt{1 - (f_p/f)^2}$, for every case of different bias voltage. Fig. 3 shows the wavelength λ_V for the dc bias voltage V normalized by the wavelength $\lambda_{V=0}$ for $V = 0$ at $f_p = 150, 210$, and 265 MHz. Fig. 3 indicates that the wavelength becomes

short with a decrease in the bias voltage of the antenna, namely, with an increase in the thickness of the ion sheath. This phenomenon can be explained quantitatively by the following simple theoretical model: an infinitely long conducting cylinder of radius a with an insulating layer of a coaxial cylindrical vacuum sheath of radius b is immersed in a homogeneous cold plasma of infinite extent. The electromagnetic propagation constant k along this structure can be found as follows:

$$s_0^2 \left(1 - \frac{f_p^2}{f^2} \right) \ln \frac{b}{a} = s_e^2 \left(\ln \frac{s_e b}{2} + j \frac{\pi}{2} \right) \quad (1)$$

under the conditions $|s_0 b| \ll 1$ and $|s_e b| \ll 1$, where s_0 and s_e are the transverse propagation constants defined by $s_0 = \sqrt{k_0^2 - k^2}$ and $s_e = \sqrt{k_e^2 - k^2}$ in the regions of the sheath and the plasma, respectively. The dispersion equation given by (1) is analogous to that for the Goubau line. In Fig. 4 the wavelength on the wire calculated by using (1) is plotted versus the thickness of the sheath. This result indicates that the wavelength becomes short with the increasing thickness of the sheath. It is noted here that the above simple calculation shows that the equivalent relative thickness of the ion sheath b/a is about 3.5 at $f_p = 265$ MHz and $V = -32$ [V] under the assumption that $b/a = 1.0$ at $V = 0$ [V] and is equivalent to 8 times the Debye length calculated by using the electron density and the temperature.

SLOW SURFACE WAVE MODE

Similar measurements for the antenna grounded to the image plane were carried out at the frequency of 108 MHz in the region of $f_p > f$. As a result, the slow propagation mode along the antenna was observed in this cutoff region of the electromagnetic wave. In Fig. 5 the measured wavelength is plotted versus the plasma frequency. The above experimental fact can be explained by using the same theoretical model mentioned in the preceding section. Fig. 5 shows the wavelength of the slow surface wave mode along an infinitely long sheathed

cylinder calculated also by using (1). A fairly good correspondence is seen between the theory and the experiment. This surface wave mode is found to exist in a region of $f < f_p/\sqrt{2}$, and to approach to the TEM coaxial mode when f_p increases infinitely.

ACKNOWLEDGMENT

The authors would like to thank Prof. K. Kamiryo for his helpful suggestions and H. Ishikawa and K. Miyazaki for their assistance in carrying out the experiments.

T. ISHIZONE

K. TAIRA

S. ADACHI

Y. MUSHIAKE

Dept. of Elec. Comm. Engrg.

Tohoku University

Sendai, Japan

REFERENCES

- [1] H. Judson and K. M. Chen, "Measurement of antenna current distributions in a hot plasma," *Proc. IEEE (Letters)*, vol. 56, pp. 753-754, April 1968.
- [2] C. Y. Ting, B. Rao, and W. A. Saxton, "Theoretical and experimental study of a finite cylindrical antenna in a plasma column," *IEEE Trans. Antennas and Propagation*, vol. AP-16, pp. 246-255, March 1968.

Corrections:

The Field Pattern of a Long Antenna with Multiple Excitations¹

On page 644 the factor e^{2ikz} in the expression of $Y_3(z)$ should have been dropped.

LIANG-CHI SHEN

Dept. of Elec. Engrg.

University of Houston

Houston, Tex. 77004

Manuscript received March 10, 1969.

¹IEEE Trans. Antennas and Propagation, vol. AP-16, pp. 643-646, November 1968.

Radiation and Near-Field Coupling Between Two Collinear Open-Ended Waveguides¹

Equation (1) should have read

$$\vec{E}(r) = -j\omega \nabla \times \vec{U}_m. \quad (1)$$

In equation (10) the first expression in parentheses should have read

$$(e^{j\gamma_{10}z} - \Gamma e^{-j\gamma_{10}z}).$$

In Fig. 6(b) parameter $d = 1.35''$ should have read $d = 1.25''$.

ROBERT J. MAILLOUX

NASA Electron. Res. Ctr.

Cambridge, Mass. 02139

Manuscript received April 25, 1969.

¹IEEE Trans. Antennas and Propagation, vol. AP-17, pp. 49-55, January 1969.

A Creeping-Wave Analysis of the Edge-On Echo Area of Disks¹

Equation (2) should have read

$$\alpha = 0.21 e^{j\pi/6} \rho^{-2/3} \lambda^{-1/3} \quad (2)$$

to agree with the $e^{j\omega t}$ time convention used.

CHARLES E. RYAN, JR.

LEON PETERS, JR.

ElectroScience Lab.

Ohio State University

Columbus, Ohio 43212

Manuscript received May 23, 1969.

¹IEEE Trans. Antennas and Propagation (Communications), vol. AP-16, pp. 274-275, March 1968.